Using physiologically based pharmacokinetic (PBPK) modeling for dietary risk assessment of titanium dioxide (TiO 2) nanoparticles

Article *in* Nanotoxicology · July 2014

DOI: 10.3109/17435390.2014.940404 · Source: PubMed

3 authors, including:

Gerald Bachler
PFA Brussels sprl
7 PUBLICATIONS **159** CITATIONS
SEE PROFILE

Natalie Von Goetz
Bundesamt für Gesundheit, Schweiz
74 PUBLICATIONS **2,348** CITATIONS
SEE PROFILE

http://informahealthcare.com/nan
ISSN: 1743-5390 (print), 1743-5404 (electronic)

Nanotoxicology

Nanotoxicology, Early Online: 1–8
 DOI: 10.3109/17435390.2014.940404

informa
healthcare

ORIGINAL ARTICLE

Using physiologically based pharmacokinetic (PBPK) modeling for dietary risk assessment of titanium dioxide (TiO_2) nanoparticles

Gerald Bachler, Natalie von Goetz, and Konrad Hungerbuhler

ETH Zurich, Institute for Chemical and Bioengineering, Zurich, Switzerland

Abstract

Nano-sized titanium dioxide particles (nano-TiO_2) can be found in a large number of foods and consumer products, such as cosmetics and toothpaste, thus, consumer exposure occurs via multiple sources, possibly involving different exposure routes. In order to determine the disposition of nano-TiO_2 particles that are taken up, a physiologically based pharmacokinetic (PBPK) model was developed. High priority was placed on limiting the number of parameters to match the number of underlying data points (hence to avoid overparameterization), but still reflecting available mechanistic information on the toxicokinetics of nano-TiO_2. To this end, the biodistribution of nano-TiO_2 was modeled based on their ability to cross the capillary wall of the organs and to be phagocytosed in the mononuclear phagocyte system (MPS). The model's predictive power was evaluated by comparing simulated organ levels to experimentally assessed organ levels of independent *in vivo* studies. The results of our PBPK model indicate that: (1) within the application domain of the PBPK model from 15 to 150 nm, the size and crystalline structure of the particles had a minor influence on the biodistribution; and (2) at high internal exposure the particles agglomerate *in vivo* and are subsequently taken up by macrophages in the MPS. Furthermore, we also give an example on how the PBPK model may be used for risk assessment. For this purpose, the daily dietary intake of nano-TiO_2 was calculated for the German population. The PBPK model was then used to convert this chronic external exposure into internal titanium levels for each organ.

Keywords

Biodistribution, E171, German population, PBTK model, toxicokinetics

History

Received 28 January 2014
Revised 19 June 2014
Accepted 27 June 2014
Published online 24 July 2014

Introduction

While titanium was first discovered in 1791, it took until the 1920s to establish production processes for large quantities of pigment titanium dioxide (TiO_2) of high purity (96% to 99%) (Laver, 1997). Back in the 1920s, TiO_2 particles were mainly used in paints, but also in pastels, inks, papers, ceramics, glass and leather goods (Laver, 1997). Nowadays, TiO_2 particles are widely used in a broad range of food and consumer products, such as cosmetics, textiles, sweets and toothpastes (von Goetz et al., 2013; Weir et al., 2012). This wide usage can be attributed to the brightness and very-high refractive index of TiO_2 particles. These properties turn TiO_2 into an effective UV light absorber and the pigment with the highest production volume in the world (Baan et al., 2006; Jin & Berlin, 2007). The size of the TiO_2 particles produced determines whether they are used as UV light absorber or as a pigment. Below a size of 100 nm, TiO_2 particles appear transparent on the skin, which makes nano-sized TiO_2 particles (nano-TiO_2) very popular for the use in cosmetics (US-EPA, 2010). In fact, in 2005 two-thirds of the world's nano-TiO_2 production of approximately 2000 metric tons were used in cosmetics (US-EPA, 2010). If the particle size is larger than the nano-scale, TiO_2 particles (conventional TiO_2) scatter the visible light to a much higher degree and therefore appear white. However, as recently shown by Weir et al. (2012), also white pigment samples may contain a significant proportion of particles in the nano-range. Weir et al. determined the size distribution of food-grade TiO_2 (in the following denoted as ''E171'') and could show that by number approximately 36% of the particles had at least one dimension below 100 nm.

The extensive usage of TiO_2 can also be attributed to the fact that conventional TiO_2 is considered to be of low toxicity (Shi et al., 2013). For example, the European Food Safety Authority (EFSA) concluded that TiO_2, in both commercially relevant crystalline forms (rutile and anatase), does not pose any safety concern and accordingly no limit is specified for the acceptable daily intake (ADI) by the Joint FAO/WHO Expert Committee Report on Food Additives (JECFA) (EFSA, 2004). However, the EFSA evaluation did not specifically include nano-TiO_2, even if E171 might contain considerable amounts of particles in the nano-range.

The usage of nano-TiO_2 in many products has raised concerns about possible adverse effects on human health. These concerns originate from the considerably different physicochemical and biological behavior of nano-TiO_2 as compared to conventional TiO_2, e.g. an increased photo-catalytic activity due to an increased surface area (Jiang et al., 2008) or the ability to cross the cell membrane more easily (''Trojan Horse effect'', Kreuter, 2004). Additionally, the discussion on the carcinogenicity of inhaled conventional TiO_2 (ILSI Risk Science Institute Workshop Participants, 2000; Lee et al., 1985) draws the attention to possible health effects caused by exposure to nano-TiO_2 (Oberdorster et al., 1994; Sager et al., 2008). Hence, efforts are

Correspondence: Natalie von Goetz, ETH Zurich, Institute for Chemical and Bioengineering, Vladimir-Prelog-Weg 1-5, 8093 Zurich, Switzerland. Tel: +4144 6320975. E-mail: natalie.von.goetz@chem.ethz.ch

undertaken to improve the knowledge on the toxicity and toxicokinetics (TK) of nano-TiO_2 (Shi et al., 2013).

One method that can be used to structure available TK data and hence gain deeper insight in the biodistribution of chemical substances is physiologically based pharmacokinetic (PBPK) modeling (Nestorov, 2007). PBPK models are usually designed as multi-compartment models that aim to describe the absorption, distribution, metabolism and excretion (ADME) of chemical substances in an organism by a system of differential equations. Each compartment represents a defined part of the organism, such as a group of organs/tissues (e.g. slowly perfused tissue) or a single organ/tissue (e.g. liver) or a region of an organ/tissue (e.g. intracellular space). Hence, PBPK models can help to determine the ADME of chemical substances and provide insight into the relationships between external exposure and internal exposure of different organs/tissues (IPCS, 2010). Yet, for nanoparticles (NPs) only a handful of published PBPK models are available in the literature. The number of models that could be validated against independent data is even lower: To our knowledge, validated PBPK models are only available for poly(lactic-co-glycolic) acid (PLGA; Li et al., 2012) and silver (Bachler et al., 2013) NPs.

In order to contribute to the current effort to improve the understanding of the TK of nano-TiO_2 and relate external exposure from various sources to internal exposure, we have developed a PBPK model for nano-TiO_2. The predictive capability of the PBPK model was evaluated by comparing predicted organ titanium levels with independent *in vivo* data.

Furthermore, to give an example on how the PBPK model may be used for risk assessment, we have determined the exposure to nano-TiO_2 for the German population and by applying the PBPK model estimated corresponding organ titanium levels. We have focused on the ingestion of nano-TiO_2, since dermal uptake of nano-TiO_2 is considered negligible (SCCS, 2013) and inhalation uptake was insignificant in animal studies (BAuA, 2013; van Ravenzwaay et al., 2009). The ingestion of nano-TiO_2 was calculated on the basis of three main product groups: (1) foods and beverages (F&B), (2) drugs and dietary supplements (DDS) and (3) toothpastes (TP).

Methods

PBPK model development

The PBPK model for nano-TiO_2 (Figure 1) was developed in analogy to a recently presented PBPK model for silver NPs (Bachler et al., 2013). A detailed description of the structure of the PBPK model can be found in the Supplementary material (Section 1). Here, we give a short overview and discuss the modifications that were implemented for nano-TiO_2.

The model has an application domain of 15 to 150 nm and describes the biodistribution of NPs on the basis of two major kinetic processes. As shown for silver NPs, the biodistribution of NPs is mainly governed by (1) the ability of NPs to cross the capillary wall of the organs and (2) to be phagocytosed in the mononuclear phagocyte system (MPS). In the PBPK model, both processes are considered simultaneously, by the introduction of separate compartments in organs where the MPS is primarily located (i.e. liver, lung and spleen; van Furth et al., 1972). The compartment model was calibrated with data from Xie et al. (2011), who investigated the TK of intravenously administered 20 nm large rutile nano-TiO_2 at a dose of 10 mg/kg body weight (b.w.) in a murine model.

The transportation of NPs from the blood to the tissue compartments and excrements was described by a membrane-limited model (Li et al., 2010). Therefore, the translocation rate $k_{trans\_blood\_organ}$ (min^{-1}) of nano-TiO_2 from the blood to the different organs, bile and urine was calculated according to the following equation:

$$k_{trans\_blood\_organ} = b_{trans\_constant\_organ} \times \frac{Q_{organ\_blood}}{V_{blood}} \quad (1)$$

where $b_{trans\_constant\_organ}$ [-] represents the nanoparticulate translocation constants of the organs, which were calibrated with data from Xie et al. (2011), Q_{organ_blood} [l/min] is the flux of blood through the organ and V_{blood} [l] is the total blood volume in the body.

For the transcapillary pathway, $b_{trans\_constant\_organ}$ (Equation 1) represents the permeability of the capillary wall. For organs with the same capillary wall type (CT) the same translocation constant $b_{trans\_constant\_organ}$ was used. In total five CT groups were formed, a list of which can be found in the supplementary material (Table S3). The excretion of nano-TiO_2 was hypothesized to occur also via the transcapillary pathway. Thus, Equation 1 was used to model the excretion of the NPs via the biliary and urinary route.

Unlike the transcapillary pathway, the uptake of NPs by the MPS seems to depend on particle size (Lankveld et al., 2010) and dose (Kim et al., 2008). Hence, $b_{trans\_constant\_organ}$ should be particle and dose specific; however, no such data exists.

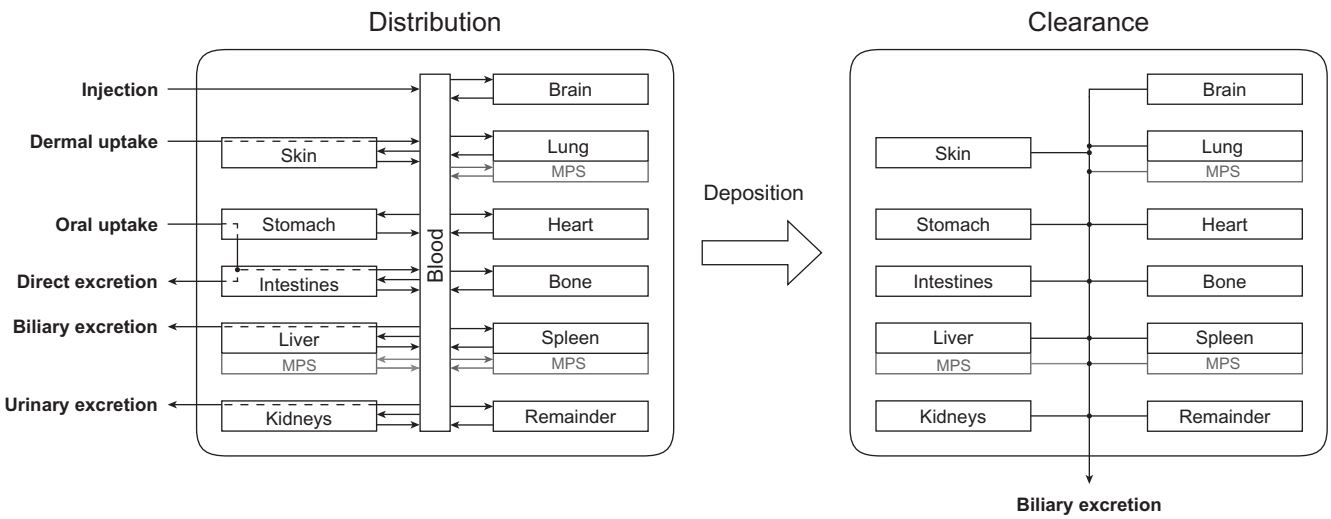

Figure 1. Schematic diagram of the nano-TiO_2 PBPK model (Dashed lines symbolize the translocation of NPs through the different biological barriers. Direct excretion represents NPs that are not absorbed in the intestines after oral exposure. Clearance compartments represent NPs that temporarily deposit in the organs and from which they are slowly cleared via the biliary route – see main text).

Therefore, the MPS translocation constants that were determined with the data of Xie et al. (2011) are only valid for similar particle sizes (20 nm) and doses (10 mg/kg b.w.), which among the studies that were used to validate the PBPK model, was only true for the study conducted by Fabian et al. (2008). However, the other studies (Wang et al., 2007a; Wu et al., 2009) were conducted with very low doses where the uptake by the MPS is negligible (Bachler et al., 2013). Hence, for the validation with the other *in vivo* studies and the dietary exposure assessment, uptake by the MPS compartments was not considered.

In contrast to silver NPs, nano-TiO_2 particles are very stable and dissolution is minimal, even at low pH and body temperature (Schmidt & Vogelsberger, 2006), and therefore dissolution kinetics were not implemented in this model. Furthermore, since TiO_2 particles are considered to be non-accumulative (EFSA, 2004), compartments were included where nano-TiO_2 temporarily deposits and is then slowly cleared via the biliary route (Figure 1). The physiological background of the slow clearance (half-life approx. 1 month) of parts of the nano-TiO_2 is unknown, but this behavior might be related to a temporary internalization of NPs by cells in the organs (e.g. leukocytes).

As for silver NPs, the amount of TiO_2 that could be recovered from the organs and excrements in the *in vivo* study was considerably lower than the dose of nano-TiO_2 that was administered via intravenous injection into the mice (Xie et al., 2011). In the nano-TiO_2 PBPK model we therefore introduced a ''Remainder'' compartment, which represents all tissues and organs that are not covered by any other compartment and to which the NPs are transported that could not be assigned to any other compartment. Furthermore, the amount of titanium that was recovered from urine by Xie et al. is unusually high. As shown by Choi et al. (2007), the renal clearance of quantum dots is limited to particles that are smaller than 5 to 6 nm. This cut-off size, however, is much smaller than the 20 nm TiO_2 particles that were used by Xie et al. In fact, above this threshold of 6 nm the urinary excretion of various metal and metal oxide NPs, including nano-TiO_2, is usually reported to be insignificant (Baek et al., 2012; Dziendzikowska et al., 2012; Hirn et al., 2011, Shinohara et al., 2014; Semmler-Behnke et al., 2008). In contrast, it is known that iodine, which was used to label the NPs, is excreted almost exclusively via urine (ATSDR, 2004). Thus, we assumed that the high urinary levels are related to the excretion of detached iodine (e.g. due to poor attachment efficiency or to the detachment of the iodine *in vivo*) and adjusted the kinetic parameters accordingly. More information on the parameterization of the kinetic rates can be found in the supplementary material (Section 2).

Finally, we conducted an uncertainty analysis for all calculations with the PBPK model. We carried out a Monte Carlo simulation (1000 iterations) with model parameters changed randomly in each iteration within their given distributions. To this end, log-normal distributions were used for the physiological and compound-dependent parameters. A full list of parameters, along with the associated equations is given in the supplementary material (Section 3).

Comparison with independent data

The predictive capability of the PBPK model was evaluated by reproducing the exposure scenario of *in vivo* experiments and comparing simulated results to experimentally assessed organ levels. Dermal and oral absorption fractions were fitted by minimizing the differences between simulated and experimentally assessed organ levels reported in Wu et al. (2009) and Wang et al. (2007a) with the least squares method, respectively.

Dietary intake and exposure assessment

The dietary titanium intake of the German population was determined for six different age classes and on the basis of three main product groups (F&B, DDS and TP), which were further divided into 83 subgroups (63 F&B, up to 19 DDS and one TP subgroups). In general, conservative parameters were chosen. The German population was taken as a model population because good quality data was available both for dietary and drug intake. The age classes are consistent with the EFSA Comprehensive European Food Consumption Database (EFSA, 2011): ''Toddlers'' (1–2 years), ''Other Children'' (3–9 years), ''Adolescents'' (10–17 years), ''Adults'' (18–64 years), ''Elderly'' (65–74 years) and ''Very Elderly'' (75+ years). Intake rates of the 83 product subgroups were taken from the literature, national health studies, market surveys and the EFSA Comprehensive European Food Consumption Database. The information on the titanium content of the 83 product subgroups was also taken from the literature. However, since the actual form of the titanium in the products has not been determined in any study, the assessment was carried out for total titanium intake. From these results the E171 and nano-TiO_2 intake was calculated on the basis of the ratio of ionic to particulate titanium intake and the amount of nano-TiO_2 in E171. The approach for each product group is discussed in detail in the supplementary material (Section 4). In general, the Monte Carlo method was used to estimate the ingestion of titanium for each age group (50 000 iterations), using Bernoulli, uniform and log-normal distributions. For deriving the distributions, non-detects were replaced by half the limit of detection (GEMS/Food-EURO, 1995). The intestinal absorption fraction was derived as described in the section above.

Results

PBPK model development

Using a previously developed approach and model structure (Bachler et al., 2013), a PBPK model for nano-TiO_2 was established. In Figure 2(A–E), the results of the model calibration with the data of Xie et al. (2011) are depicted. The organ titanium levels of the PBPK model are all higher than the ones measured by Xie et al., the reason we believe being that the iodine used to label the NPs was partly detached from the NPs. However, the calibration results fall near to the 1:1 line that has been corrected by a factor of 3.9 to account also for the detached iodine: i.e. all organ titanium levels at all points in time are in good agreement with the data of Xie et al. Sole exceptions are the intestines, where the uptake of nano-TiO_2 is overestimated by the PBPK model at all points in time. This might be caused either by an increased translocation of nano-TiO_2 from the enterocytes to the blood circulation *in vivo* or to a direct intestinal excretion of nano-TiO_2 by the enterocytes. However, since the physiological mechanism is unclear, we have deliberately not included these kinetics into the PBPK model.

More results on the calibration process can be found in the supplementary material (Section 2). Also, the results from the sensitivity analysis for the human PBPK model can be found in the supplementary information (Section 5).

Comparison with independent data

The applicability of the PBPK model was evaluated by comparing organ titanium levels to three independent *in vivo* studies. To assess the potential of the PBPK model to be extrapolated to other particle sizes, species and routes of administration, data of various particle sizes, from various animal models (mice and rats) and after intravenous, oral and dermal administration was used for the evaluation.

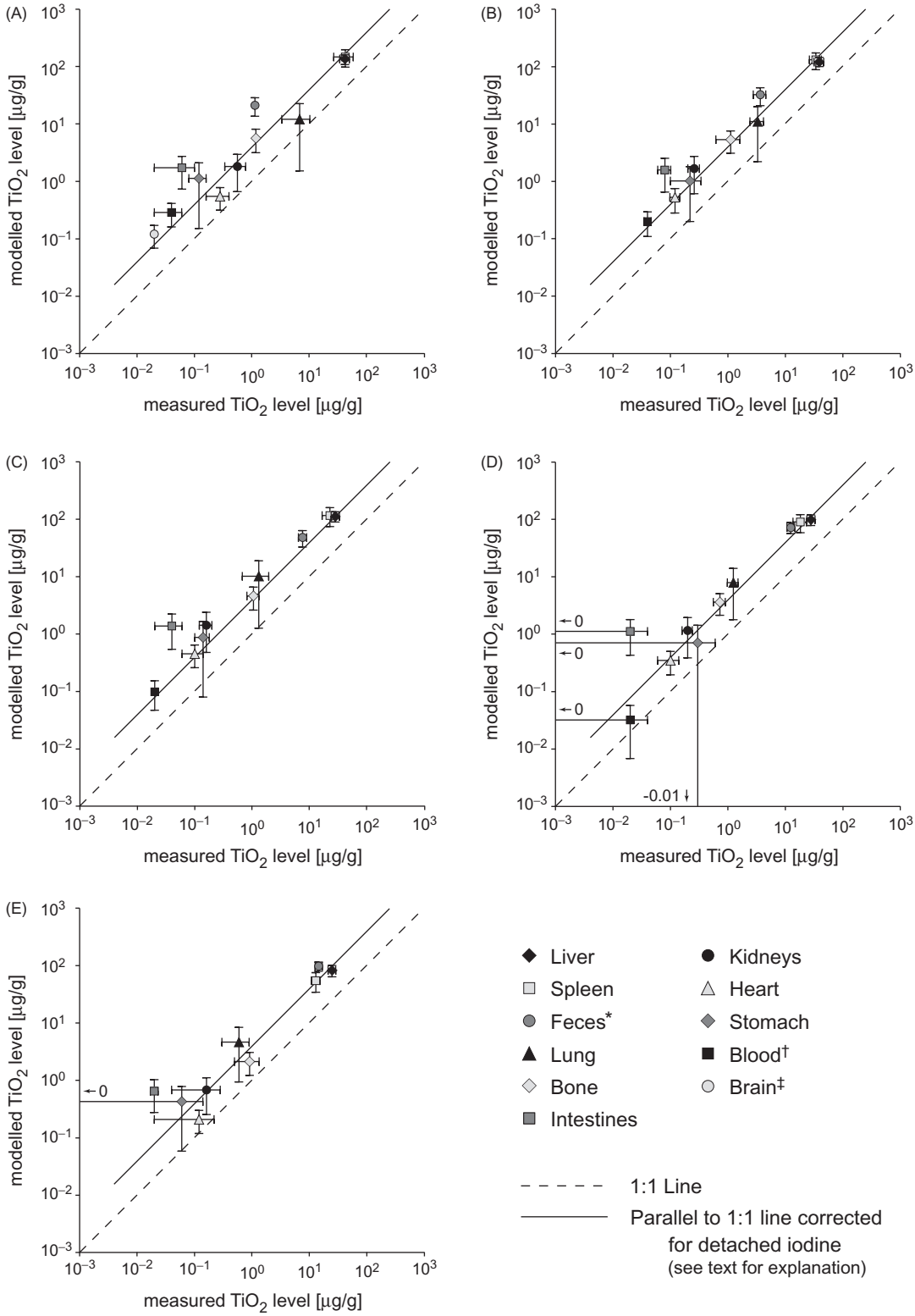

Figure 2. Results of the PBPK model calibration with the data of Xie et al. (2011). (A) 1 day, (B) 3 days, (C) 7 days, (D) 15 days and (E) 30 days after the intravenous injection of 20 nm large rutile TiO_2 particles at a dose of 10 mg/kg b.w. (*in µg; †below limit of detection at day 30; ‡below limit of detection at day 3, 7, 15 and 30; error bars represent standard deviation, $n = 5$ (*in vivo*), $n = 1000$ iterations (PBPK model)).

First, the PBPK model was compared to *in vivo* data from Fabian et al. (2008), who intravenously administered uncoated 20 to 30 nm large TiO_2 particles to rats. The nano-TiO_2 consisted of both anatase and rutile forms (70/30). As can be seen in Figure 3, nearly all organ levels at all points in time could be successfully predicted by the PBPK model. Solely the kidney levels at ''Day 1'' are slightly above the 1:1 line.

In a second step, we compared the PBPK model to organ levels from orally exposed mice (Figure 4A). In the *in vivo* study, the mice were exposed once to 5 g/kg b.w. uncoated rutile particles (25 and 80 nm) and were sacrificed two weeks later (Wang et al., 2007a, 2008). The intestinal absorption fraction was determined with our PBPK model to be $0.060 \pm 0.034\%$ for both 20 and 80 nm particles. For most organs the predicted titanium levels are very

close to the experimentally assessed levels, except for the liver, where there is a considerable discrepancy, especially for the 80 nm particles. The high liver levels for 80 nm particles might be explained by agglomerates that are formed in the stomach by contact with gastric acid (Peters et al., 2012; Walczak et al., 2013) and are not dispersed again in the intestinal tract. In the small intestines, agglomerates up to 20 μm may be absorbed into the blood circulation through Peyer's patches (Hagens et al., 2007). These absorbed agglomerates first pass through the liver and then the lung before they are distributed to the rest of the body. Due to their increased size, however, these agglomerates are probably much more effectively taken up by macrophages in these two organs (Champion et al., 2008, van Furth et al., 1972). Hence, this hypothesis would not only explain the extremely elevated liver titanium levels but also the slightly higher titanium levels of the lung *in vivo* as compared to the PBPK model (Figure 4A), where these kinetics had not been implemented.

In a last step, the PBPK model was used to predict the organ titanium levels after the dermal application of nano-TiO_2 (Figure 4B). We used the study of Wu et al. (2009), who dermally applied 1200 μg/day uncoated anatase/rutile (75/25) NPs of 21 nm, uncoated rutile NPs of 25 nm and uncoated rutile NPs of 60 nm, respectively, on the dorsal skin in the interscapular of BALB/c hairless mice for 60 days. The percutaneous absorption fraction was determined with our PBPK model to be $3.6 \pm 1.8\%$. Most predicted titanium levels agree reasonably well with the experimental data. However, the titanium levels of the kidneys are considerably overestimated by the PBPK model for all particle sizes. One possible explanation might be that active transport processes play no role in the dermal uptake of NPs. Hence, smaller-sized particles (within the size distribution of the used NPs) translocate easier through the skin and are probably preferentially taken up (Sonavane et al., 2008). These small particles, however, can easily pass the relative large pores of the capillary walls of the kidneys (Table S3), which enhances the translocation of NPs from the blood to the urine. Furthermore, for the 21 nm particles there is a discrepancy of the lung and brain titanium levels between the PBPK model results and the *in vivo* data. These differences also might be related to the higher dermal uptake of smaller particles compared to larger particles. Since they can pass more easily through the pores of the blood capillaries (Table S3), they are distributed much more homogeneously in the body, which is not reflected in the PBPK model.

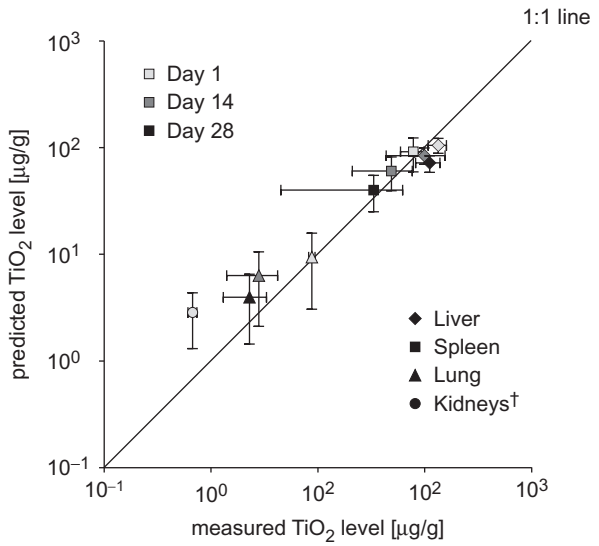

Figure 3. Comparison of the PBPK model to toxicokinetic data from Wistar rats 1, 14 and 28 days after intravenous injection of uncoated 20–30 nm large TiO_2 particles at a dose of 5 mg/kg b.w. (Fabian et al., 2008) (†below limit of detection at Day 14 and 28; error bars represent standard deviation, $n = 3$ (*in vivo*), $n = 1000$ iterations (PBPK model)).

Dietary intake and exposure assessment

Figure 5 shows the dietary intake of titanium as calculated for the German population. The daily median intake is between 0.5 and 1.0 mg/kg b.w. for all age groups except the age group ''Other Children'', who have the highest titanium intake of all age classes (approximately 2.0 mg/kg b.w.). Common for all age classes is the high variability in the titanium intake.

For ''Adults'' the eight product subgroups that contribute most to the ingestion of titanium are summarized in Figure 6(A). In Figure 6(B), organ titanium levels that result from the daily intake of nano-TiO_2 (95th percentile) are depicted for ''Adults''. In total, it was assumed that 10% of the total titanium intake is in the nano-range, which is a conservative estimation based on the ratio of ionic to particulate titanium intake (1:19) and the amount of nano-TiO_2 in E171 (approximately 11% by weight) (Weir et al., 2012). We used four times the value that we determined from the *in vivo* study of Wang et al. (2007a) as the intestinal absorption fraction. The safety factor of four was based on the results of the

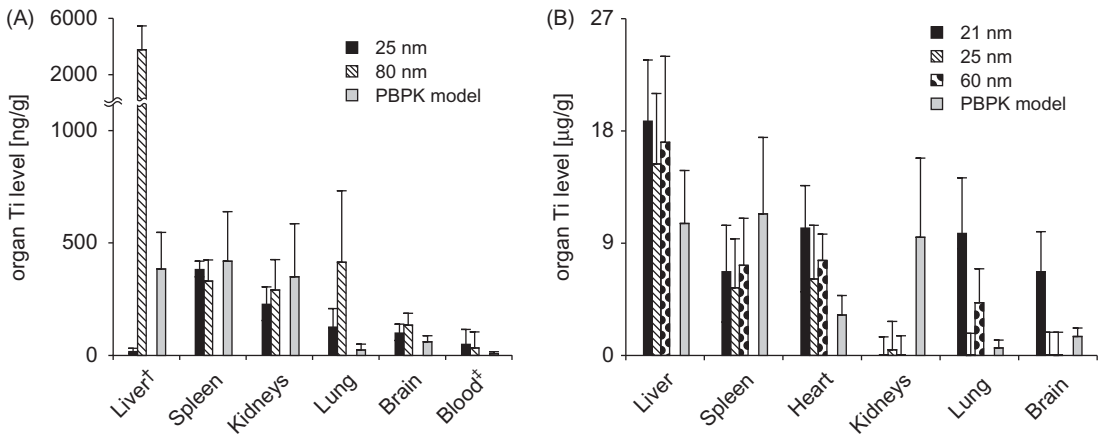

Figure 4. Comparison of the PBPK model to toxicokinetic data of mice. (A) Two weeks after the oral administration of 5 g/kg b.w. uncoated rutile TiO_2 nanoparticles to CD-1 (ICR) mice (Wang et al., 2007a). (B) After 60 days of daily dermal application of 1200 μg uncoated TiO_2 nanoparticles on the dorsal skin in the interscapular of BALB/c hairless mice (Wu et al., 2009). (†the extremely deviating liver levels were not included in the determination of the intestinal absorption fraction; ‡*in vivo* data represents the titanium levels in red blood cells; the organ titanium levels of the *in vivo* studies were background corrected; error bars represent standard deviation, $n = 6$ to 20 (*in vivo*), $n = 1000$ iterations (PBPK model)).

silver PBPK model, where we could show that the intestinal absorption fraction at low ingestion doses may be up to four times higher compared to high ingestion doses (Bachler et al., 2013).

The most important product subgroups and the calculation of the biodistribution of nano-TiO_2 for the other age classes can be found in the supplementary material (Section 4).

Discussion

PBPK model development

The biodistribution of nano-TiO_2 could be modeled on the basis of their ability to cross the capillary walls of the organs and to be phagocytosed in the MPS. The permeability of the different capillary wall types was similar for the nano-TiO_2 PBPK model and silver NPs PBPK model, which indicates that (1) the capillary wall type is one of the most crucial factors that determine the biodistribution of NPs and (2) that metal and metal oxides NPs behave similarly *in vivo*.

We used the data of Xie et al. (2011) for the calibration of the PBPK model, because it is, next to the study of Shinohara et al. (2014), by far the most comprehensive *in vivo* study on nano-TiO_2 in the literature, both regarding evaluated organs and time points. The study of Shinohara et al. was not considered because their dosage circumvents validation with the data of Fabian et al. (2008). However, one limitation of the data set of Xie et al. (2011) is the extremely high urinary excretion rate that we assumed is related to the excretion of detached iodine. Although the stability of iodine-labeled NPs is not specifically discussed in literature, the comparison of the organ levels that were simulated with the PBPK model corrected for detached iodine to organ levels determined in an independent *in vivo* study (Fabian et al., 2008) supports the assumption that a large fraction of the iodine was not attached to the nano-TiO_2. Furthermore, it has been reported that after the intravenous injection of nano-TiO_2 in male ddY mice, the liver level decreased by approximately 30% within one month (Sugibayashi et al., 2008), which is similar to the 38% that can be observed in the simulation. Nevertheless, it cannot be excluded that the detachment of iodine occurs only in a particular part of the body and, hence, the nano-TiO_2 that lost their iodine label may accumulate in a specific compartment. For example, the detachment of iodine may occur mainly in the acidic environment of macrophages that try to digest them. An alternative parameterization approach on the basis of this assumption can be found in the supplementary material (Section 2).

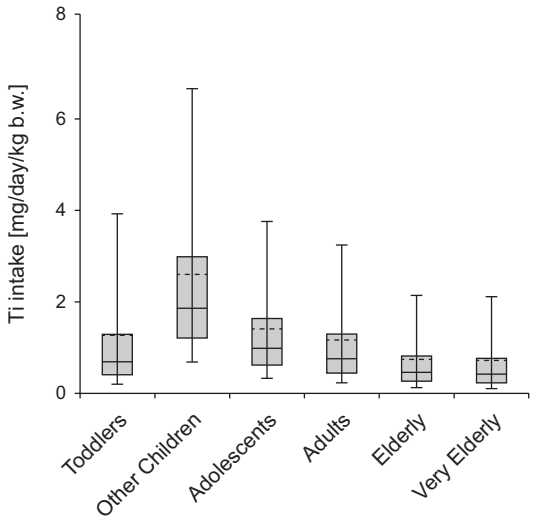

Figure 5. Box plot of the titanium ingestion rates for the six different age classes of the German population. (Continuous and dashed lines represent the median and average intake, respectively; boxes represent 25th and 75th percentiles; whiskers represent 5th and 95th percentiles.)

Comparison with independent data

The PBPK model could predict most of the organ titanium levels of the independent *in vivo* studies. Discrepancies in the liver levels after oral administration and in the kidney levels after dermal application are probably related to the uptake of agglomerates and NPs smaller than 15 nm, respectively. Both particle sizes are outside the application domain of the PBPK model, which is from 15 to 150 nm. Nevertheless, these results suggest that it is possible to use the PBPK model for different particle sizes, species and routes of administration. The sole limitation of the model is that it is not possible to extrapolate from low to high doses. This is mainly due to the complex uptake kinetics of NPs by the MPS, which seems to be dose (Kim et al., 2008) and, at high doses, also size (Lankveld et al., 2010) dependent. The physiological background of this behavior still needs to be determined, but the results of our PBPK models (silver NPs and nano-TiO_2) suggest that there is a threshold concentration in the blood that triggers the uptake of NPs by the MPS. Two possible

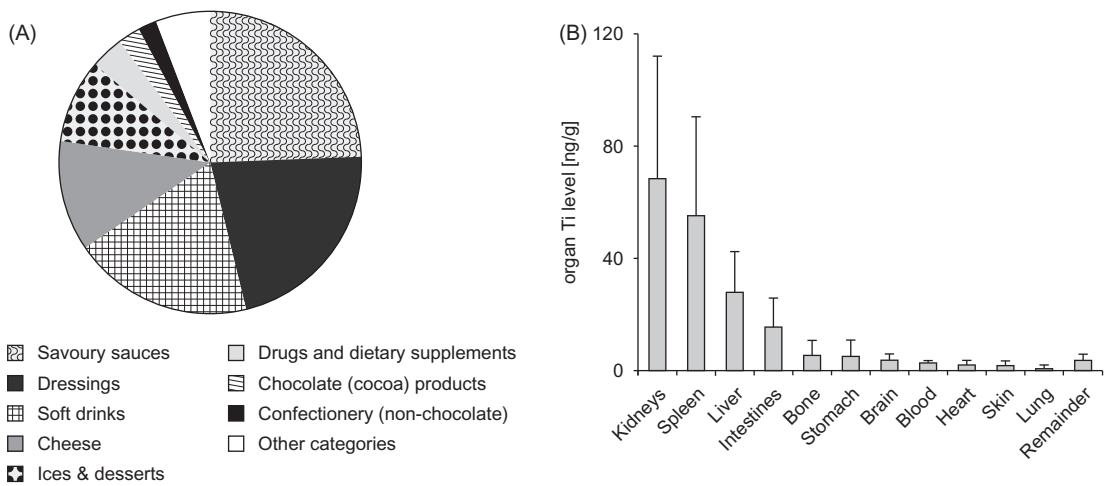

Figure 6. (A) The top eight subgroups that contribute most to the total titanium intake in ''Adults''. (B) Steady-state organ levels of nano-TiO_2 that are ingested daily by ''Adults'' (for the nano-TiO_2 intake the 95th percentile from Figure 5 was used, error bars represent standard deviation, $n = 1000$ iterations).

explanations might be (1) the agglomeration of NPs or (2) a substantial alteration of the protein corona due to a deficit of available proteins at high doses. Both processes have the ability to increase the uptake of NPs by macrophages. Agglomerates have a size that is much closer to the maximum phagocytosis efficiency of macrophages, which is around 3 µm (Champion et al., 2008), and, indeed, *in vivo* agglomerates of NPs are very often observed in macrophages (BAuA, 2013; Hirn et al., 2011; Loeschner et al., 2011; van Ravenzwaay et al., 2009). On the other hand, the composition of the protein corona has a large influence on the recognition of NPs by the immune system (Saptarshi et al., 2013) and might also promote agglomeration of NPs (Xu et al., 2004). Nevertheless, at low internal doses, when NPs are only gradually translocated to the blood via the epithelial layer of the lung, intestines or skin, this effect seems to play no significant role. In fact, under these conditions the best results with our PBPK models are obtained if an uptake by the MPS compartments is not considered.

The intestinal absorption fraction that we determined with our PBPK model is very similar to the fraction that was determined with the PBPK model for silver NPs after the oral administration of high doses to rats (0.12%; Bachler et al., 2013). Unfortunately, absorption fractions for nano-TiO_2 (*in vitro* and *in vivo*) that may be directly compared to our results are lacking in the literature.

We determined a percutaneous absorption fraction of over 3% for dermal application of nano-TiO_2, which is relatively high. In fact, in other *in vitro* and *in vivo* studies the dermal uptake is usually reported as insignificant (SCCS, 2013). The reason for this discrepancy might be related to the fact that Wu et al. (2009) used uncoated nano-TiO_2, as compared to other studies that used commercial nano-TiO_2, which are usually coated with silica or alumina (SCCS, 2013). Another explanation might be that Wu et al. (2009) used hairless mice, which for many compounds show much higher skin permeability as compared to humans (Simon & Maibach, 1998).

Dietary intake and exposure assessment

The TiO_2 intake by ingestion that we determined for the different age groups in Germany is very similar to the results reported by Weir et al. (2012), who assessed the dietary intake of TiO_2 for the UK and the USA. Solely the intake of ''Toddlers'' is considerable lower in the German population as compared to the UK and USA, where the TiO_2 intake of ''Toddlers'' is nearly as high as of ''Other Children''.

The 95th percentile titanium organ levels after ingestion of nano-TiO_2 are below 170 ng/g for all age groups and in all organs. This value is much lower than levels for which toxic effects have been reported in the majority of *in vitro* studies (Hussain et al., 2005; Long et al., 2006; Sayes et al., 2006; Wang et al., 2007b). However, some uncertainties and conservatisms of the assessment should be noted: (1) interspecies differences in the ability of NPs to cross the capillary wall have not been determined to date; (2) a dose-dependent uptake of NPs in the intestinal tract was indicated by the PBPK model for silver NPs; (3) in the studies available, the titanium content in F&B was mainly determined in products where the authors expected high titanium levels. Hence, since products with low titanium levels are underrepresented in our assessment, the actual amount of ingested nano-TiO_2 has been overestimated.

As discussed in the Introduction, the focus of this risk assessment was on the ingestion of nano-TiO_2. However, if future studies induce the reevaluation of the dermal and/or the inhalation uptake of nano-TiO_2, these routes may easily be added to the PBPK model (Bachler et al., 2013).

Conclusion

According to this dietary exposure assessment, no organ of any age group is exposed to titanium levels where adverse effects have been reported *in vitro*. Hence, our assessment indicates that the risk from the ingestion of nano-TiO_2 via F&B, DDS and TP for the German population is small.

With the PBPK model, the biodistribution of nano-TiO_2 could be successfully described on the basis of two kinetic processes: (1) by the ability of NPs to cross the capillary wall of the organs; (2) by the phagocytosis of NPs by the MPS. However, at low levels of nano-TiO_2 in the blood, the uptake by the MPS compartments seems to be negligible. Although the reason for this behavior could not be definitively determined, the results of the PBPK model suggest agglomeration of NPs at high doses and a subsequent uptake of these agglomerates by macrophages.

The mechanistic insights that were obtained by our PBPK model may be used to indicate research priorities and inform on the design of future *in vivo* studies. The following experimental studies would help to further increase the reliability of the PBPK model and the dietary intake and exposure assessment: (1) *in vitro* determination of intestinal absorption fractions of nano-TiO_2 of different sizes, crystalline structures, coatings and concentrations; (2) interspecies and intraspecies differences in the permeability of blood capillaries to nano-TiO_2; (3) TK data on nano-TiO_2 that are smaller than 15 nm; (4) investigation of the disposition of nano-TiO_2 that could not be recovered by Xie et al. (2011).

Declaration of interest

The authors declare that there is no conflict of interest. The study was funded by the Swiss Federal Office of Public Health (FOPH).

References

ATSDR. 2004. Toxicological profile for iodine. Atlanta (GA): Agency for Toxic Substances and Disease Registry.

Baan R, Straif K, Grosse Y, Secretan W, El Ghissassi F, Cogliano V. 2006. Carcinogenicity of carbon black, titanium dioxide, and talc. Lancet Oncol 7:295–6.

Bachler G, von Goetz N, Hungerbuhler K. 2013. A physiologically based pharmacokinetic model for ionic silver and silver nanoparticles. Int J Nanomedicine 8:3365–82.

Baek M, Chung HE, Yu J, Lee JA, Kim TH, Oh JM, et al. 2012. Pharmacokinetics, tissue distribution, and excretion of zinc oxide nanoparticles. Int J Nanomedicine 7:3081–97.

BAuA. 2013. Toxic effects of various modifications of a nanoparticle following inhalation. German Federal Institute for Occupational Safety and Health: Research Project F2246. Dortmund/Berlin/Dresden, Germany.

Champion JA, Walker A, Mitragotri S. 2008. Role of particle size in phagocytosis of polymeric microspheres. Pharm Res 25:1815–21.

Choi HS, Liu W, Misra P, Tanaka E, Zimmer JP, Itty Ipe B, et al. 2007. Renal clearance of quantum dots. Nat Biotechnol 25:1165–70.

Dziendzikowska K, Gromadzka-Ostrowska J, Lankoff A, Oczkowski M, Krawczynska A, Chwastowska J, et al. 2012. Time-dependent biodistribution and excretion of silver nanoparticles in male Wistar rats. J Appl Toxicol 32:920–8.

EFSA. 2011. The EFSA comprehensive European food consumption database. [Online] Available at: http://www.efsa.europa.eu/en/datex-foodcdb/datexfooddb.htm. Accessed on August 08, 2013.

EFSA. 2004. Opinion of the scientific panel on food additives, flavourings, processing aids and materials in contact with food on a request from the commission related to the safety in use of rutile titanium dioxide as an alternative to the presently permitted anatase form. (EFSA-Q-2004-103). EFSA J 163:1–12.

Fabian E, Landsiedel R, Ma-Hock L, Wiench K, Wohlleben W, van Ravenzwaay B. 2008. Tissue distribution and toxicity of intravenously administered titanium dioxide nanoparticles in rats. Arch Toxicol 82: 151–7.

GEMS/Food-EURO. 1995. Reliable evaluation of low-level contamination of food. Report on a workshop in the frame of GEMS/Food-

EURO 26–27 May 2005, Kulmbach, Germany. World Health Organization Regional Office for Europe: EUR/ICP/EHAZ.94.12/WS04. Geneva, Switzerland.

Hagens WI, Oomen AG, De Jong WH, Cassee FR, Sips AJaM. 2007. What do we (need to) know about the kinetic properties of nanoparticles in the body? Regul Toxicol Pharmacol 49:217–29.

Hirn S, Semmler-Behnke M, Schleh C, Wenk A, Lipka J, Schaffler M, et al. 2011. Particle size-dependent and surface charge-dependent biodistribution of gold nanoparticles after intravenous administration. Eur J Pharm Biopharm 77:407–16.

Hussain SM, Hess KL, Gearhart JM, Geiss KT, Schlager JJ. 2005. In vitro toxicity of nanoparticles in BRL 3A rat liver cells. Toxicol In Vitro 19: 975–83.

ILSI Risk Science Institute Workshop Participants. 2000. The relevance of the rat lung response to particle overload for human risk assessment: A workshop consensus report. ILSI risk science institute workshop participants. Inhal Toxicol 12:1–17.

IPCS. 2010. The harmonization project document series No. 9 – Guidance on principles of characterizing and applying PBPK models in risk assessment. International Programme on Chemical Safety: WHO Library Cataloguing-in-Publication Data.

Jiang J, Oberdorster G, Elder A, Gelein R, Mercer P, Biswas P. 2008. Does nanoparticle activity depend upon size and crystal phase? Nanotoxicology 2:33–42.

Jin T, Berlin M. 2007. Titanium. In: Nordberg GF, Fowler BA, Nordberg M, & Friberg LT, eds. Handbook on the Toxicology of Metals. 3rd ed. Burlington: Academic Press, 861–70.

Kim YS, Kim JS, Cho HS, Rha DS, Kim JM, Park JD, et al. 2008. Twenty-eight-day oral toxicity, genotoxicity, and gender-related tissue distribution of silver nanoparticles in Sprague-Dawley rats. Inhal Toxicol 20:575–83.

Kreuter J. 2004. Influence of the surface properties on nanoparticle-mediated transport of drugs to the brain. J Nanosci Nanotechnol 4: 484–8.

Lankveld DP, Oomen AG, Krystek P, Neigh A, Troost-De Jong A, Noorlander CW, et al. 2010. The kinetics of the tissue distribution of silver nanoparticles of different sizes. Biomaterials 31:8350–61.

Laver M. 1997. Titanium dioxide whites. In: Fitzhugh EW, ed. Artists' Pigments: A Handbook of their History and Characteristics. Vol. 3. Washington, USA: National Gallery of Art, 295–355.

Lee KP, Trochimowicz HJ, Reinhardt CF. 1985. Pulmonary response of rats exposed to titanium dioxide (TiO_2) by inhalation for two years. Toxicol Appl Pharmacol 79:179–92.

Li M, Al-Jamal KT, Kostarelos K, Reineke J. 2010. Physiologically based pharmacokinetic modeling of nanoparticles. ACS Nano 4:6303–17.

Li M, Panagi Z, Avgoustakis K, Reineke J. 2012. Physiologically based pharmacokinetic modeling of PLGA nanoparticles with varied mPEG content. Int J Nanomedicine 7:1345–56.

Loeschner K, Hadrup N, Qvortrup K, Larsen A, Gao XY, Vogel U, et al. 2011. Distribution of silver in rats following 28 days of repeated oral exposure to silver nanoparticles or silver acetate. Part Fibre Toxicol 8: 1–14.

Long TC, Saleh N, Tilton RD, Lowry GV, Veronesi B. 2006. Titanium dioxide (P25) produces reactive oxygen species in immortalized brain microglia (BV2): implications for nanoparticle neurotoxicity. Environ Sci Technol 40:4346–52.

Nestorov I. 2007. Whole-body physiologically based pharmacokinetic models. Expert Opin Drug Metab Toxicol 3:235–49.

Oberdorster G, Ferin J, Lehnert BE. 1994. Correlation between particle-size, in-vivo particle persistence, and lung injury. Environ Health Perspect 102:173–9.

Peters R, Kramer E, Oomen AG, Rivera ZE, Oegema G, Tromp PC, et al. 2012. Presence of nano-sized silica during in vitro digestion of foods containing silica as a food additive. ACS Nano 6:2441–51.

Sager TM, Kommineni C, Castranova V. 2008. Pulmonary response to intratracheal instillation of ultrafine versus fine titanium dioxide: role of particle surface area. Part Fibre Toxicol 5:17. doi: 10.1186/1743-8977-5-17.

Saptarshi SR, Duschl A, Lopata AL. 2013. Interaction of nanoparticles with proteins: relation to bio-reactivity of the nanoparticle. J Nanobiotechnol 11:1–12.

Sayes CM, Wahi R, Kurian PA, Liu YP, West JL, Ausman KD, et al. 2006. Correlating nanoscale titania structure with toxicity: a cytotoxicity and inflammatory response study with human dermal fibroblasts and human lung epithelial cells. Toxicol Sci 92:174–85.

SCCS 2013. Opinion on titanium dioxide (nano form) – European Commision: Scientific Committee on Consumer Safety: ND-AQ-13-007-EN-N. Luxembourg.

Schmidt J, Vogelsberger W. 2006. Dissolution kinetics of titanium dioxide nanoparticles: the observation of an unusual kinetic size effect. J Phys Chem B 110:3955–63.

Semmler-Behnke M, Kreyling WG, Lipka J, Fertsch S, Wenk A, Takenaka S, et al. 2008. Biodistribution of 1.4- and 18-nm gold particles in rats. Small 4:2108–11.

Shi H, Magaye R, Castranova V, Zhao J. 2013. Titanium dioxide nanoparticles: a review of current toxicological data. Part Fibre Toxicol 10:15. doi: 10.1186/1743-8977-10-15.

Shinohara N, Danno N, Ichinose T, Sasaki T, Fukui H, Honda K, Gamo M. 2014. Tissue distribution and clearance of intravenously administered titanium dioxide (TiO_2) nanoparticles. Nanotoxicology 8:132–41.

Simon GA, Maibach HI. 1998. Relevance of hairless mouse as an experimental model of percutaneous penetration in man. Skin Pharmacol Appl Skin Physiol 11:80–6.

Sonavane G, Tomoda K, Sano A, Ohshima H, Terada H, Makino K. 2008. In vitro permeation of gold nanoparticles through rat skin and rat intestine: effect of particle size. Colloid Surface B 65:1–10.

Sugibayashi K, Todo H, Kimura E. 2008. Safety evaluation of titanium dioxide nanoparticles by their absorption and elimination profiles. J Toxicol Sci 33:293–8.

US-EPA. 2010. Nanomaterial case studies: nanoscale titanium dioxide in water treatment and in topical sunscreen – Environmental Protection Agency: EPA/600/R-09/057F. Research Triangle Park, USA.

van Furth R, Cohn ZA, Hirsch JG, Humphrey JH, Spector WG, Langevoort HL. 1972. The mononuclear phagocyte system: A new classification of macrophages, monocytes, and their precursor cells. Bull World Health Organ 46:845–52.

van Ravenzwaay B, Landsiedel R, Fabian E, Burkhardt S, Strauss V, Ma-Hock L. 2009. Comparing fate and effects of three particles of different surface properties: nano-TiO_2, pigmentary TiO_2 and quartz. Toxicol Lett 186:152–9.

von Goetz N, Lorenz C, Windler L, Nowack B, Heuberger M, Hungerbühler K. 2013. Migration of Ag- and TiO_2-(nano)particles from textiles into artificial sweat under physical stress: experiments and exposure modeling. Environ Sci Technol 47:9979–87.

Walczak AP, Fokkink R, Peters R, Tromp P, Herrera Rivera ZE, Rietjens IM, et al. 2013. Behaviour of silver nanoparticles and silver ions in an in vitro human gastrointestinal digestion model. Nanotoxicology 7: 1198–210.

Wang JJ, Sanderson BJS, Wang H. 2007b. Cyto- and genotoxicity of ultrafine TiO_2 particles in cultured human lymphoblastoid cells. Mutat Res – Genet Toxicol Environ Mutag 628:99–106.

Wang JX, Chen CY, Liu Y, Jiao F, Li W, Lao F, et al. 2008. Potential neurological lesion after nasal instillation of TiO_2 nanoparticles in the anatase and rutile crystal phases. Toxicol Lett 183:72–80.

Wang JX, Zhou GQ, Chen CY, Yu HW, Wang TC, Ma YM, et al. 2007a. Acute toxicity and biodistribution of different sized titanium dioxide particles in mice after oral administration. Toxicol Lett 168: 176–85.

Weir A, Westerhoff P, Fabricius L, Hristovski K, von Goetz N. 2012. Titanium dioxide nanoparticles in food and personal care products. Environ Sci Technol 46:2242–50.

Wu JH, Liu W, Xue CB, Zhou SC, Lan FL, Bi L, et al. 2009. Toxicity and penetration of TiO_2 nanoparticles in hairless mice and porcine skin after subchronic dermal exposure. Toxicol Lett 191:1–8.

Xie GP, Wang C, Sun J, Zhong GR. 2011. Tissue distribution and excretion of intravenously administered titanium dioxide nanoparticles. Toxicol Lett 205:55–61.

Xu Y, Linares KA, Meehan K, Love BJ, Love NG. 2004. pH dependent change in the optical properties of surface modified gold nanoparticles using bovine serum albumin. NSTI Nanotech 2004, Technical Proceedings 1:15–18.

Supplementary material available online.

Supplementary Material (Section 1–Section 5), Table S3.